Fiber confocal reflectance microscope (FCRM) for *in-vivo* imaging

Chen Liang and Michael R. Descour
Optical Sciences Center, University of Arizona, Tucson, Arizona 85721
chen.liang@optics.arizona.edu, michael.descour@optics.arizona.edu

Kung-Bin Sung and Rebecca Richards-Kortum
Biomedical Engineering, University of Texas-Austin, Austin, Texas 78712
kbsung@mail.utexas.edu, kortum@mail.utexas.edu

Abstract: *In-vivo* imaging can be achieved with a coherent-fiber-bundle based confocal reflectance microscope. Such a microscope could provide the means to detect pre-cancerous lesions in the cervix by characterizing cells' nuclear-to-cytoplasmic ratio. In this paper we present the design of such a fiber confocal reflectance microscope, with an emphasis on its optical sub-systems. The optical sub-systems consist of a commercially available microscope objective and custom designed telescope, scan lens, and coupling lens systems. The performance of the fiber confocal reflectance microscope was evaluated by imaging a resolution bar target and human cervical biopsy tissues. The results presented in this paper demonstrate a lateral resolution of 2 μm and axial resolution of 6 μm. The sensitivity of the system defined by the smallest refractive-index mismatch that can be detected is approximately $\Delta n \sim 0.05$.

OCIS codes: (170.1790) Confocal microscopy; (110.0110) Imaging systems

References and links

1 J. B. Pawley, ed., *Handbook of biological confocal microscopy*, 2nd ed. (Plenum, New York, 1995).
2 A. F. Gmitro and D. Aziz, "Confocal microscopy through a fiber-optic imaging bundle," Opt. Lett. **18**, 565-567 (1993).
3 J. Knittel, L. Schnieder, G. Buess, B. Messerschmidt, and T. Possner, "Endoscope-compatible confocal microscope using a gradient index-lens system," Opt. Comm. **188**, 267-273 (2001).
4 D. L. Dickensheets and G. S. Kino, "Silicon-micromachined scanning confocal optical microscope," J. Microelectromech. Syst. **7**, 38-47 (1998).
5 C. Williams, *Cancer biology and management: An introduction* (John Wiley & Sons Ltd., West Sussex, England, 1990).
6 C. Smithpeter, A. Dunn, R. Drezek, T. collier, and R. Richards-Kortum, "Near real time confocal microscope of cultured amelanotic cells: sources of signal, contrast agents and limits of contrast," J. Biomed. Opt. **3,** 429-436 (1998)
7 R. Drezek, T. Collier, C. Brookner, A. Malpica, R. Lotan, R. Richards-Kortum, "Laser scanning confocal microscopy of cervical tissue before and after application of acetic acid," AM J Obstet Gynecol **182**, 1135-1139 (2000).
8 A. K. Dunn, C. Smithpeter, A. J. Welch, R. Richards-Kortum, "Source of contrast in confocal reflectance imaging," Appl. Optics **38**, 2105-2115 (1999).
9 Sumitomo Electric U.S.A., Inc., Santa Clara, California, USA, http://www.sumitomoelectricusa.com.
10 L. Yang, G. Wang, J. Wang, Z. Xu, "Influence of fiber terminal face reflection on fiber optic confocal scanning microscope," in *1999 International conference on biomedical optics*, Q. Luo, B. Chance, L. V. Wang, S. L. Jacques eds., Proc. SPIE **3863**, 332-336 (1999).
11 Gradium lenses are a product of LightPath Technologies, Inc., Albuquerque, New Mexico, USA, http://www.lightpath.com.
12 MediVision Optics, Anaheim, California, USA, http://www.medivision-net.com.
13 ZEMAX is a product of Focus Software, Inc., Tucson, Arizona, USA, http://www.focus-software.com.
14 J. W. Goodman, *Introduction to Fourier Optics*, 2nd ed. (The McGraw-Hill Companies, Inc., 1996).

#37344 - $15.00 US Received October 26, 2001; Revised December 13, 2001

1. Introduction

Confocal microscopy is a well-established technique used to image a thin section within thick tissue with high lateral and axial resolution: this is known as optical sectioning [1]. An endoscopic version of a confocal microscope can be implemented with the aid of a coherent fiber bundle. Such systems have been designed and studied by several groups [2-4].

In this paper we present a near real time fiber confocal reflectance microscope (FCRM) system. The intended application of this system is to image cervical tissue *in-vivo* to detect pre-cancerous lesions. FCRM is a reflectance-based system that uses the index-of-refraction mismatch between a cell's nucleus and cytoplasm to generate an image. By examining the morphological change of a cell, characterized by its nuclear-to-cytoplasmic ratio, one can determine its normality [5]. The index mismatch between the nucleus and the cytoplasm is only approximately $\Delta n = 0.05$ [6]; this can be increased to approximately 0.07 by the application of weak acetic acid solution [7]. Index mismatches of this magnitude correspond to very low reflected signal. Therefore to achieve useful image contrast, the optical systems described in this paper are designed to maximize signal throughput relative to the background radiation [8]. Images of a resolution target are acquired with the FCRM to determine its lateral resolution for a high contrast object. Images of fresh human cervical biopsy samples are taken with the FCRM to test and demonstrate its optical sectioning capability and its functionality for the intended application.

2. Instrument overview

The FCRM is a monochromatic, epi-illuminated, point-scanning optical system. Fig. 1 shows the layout of its main components.

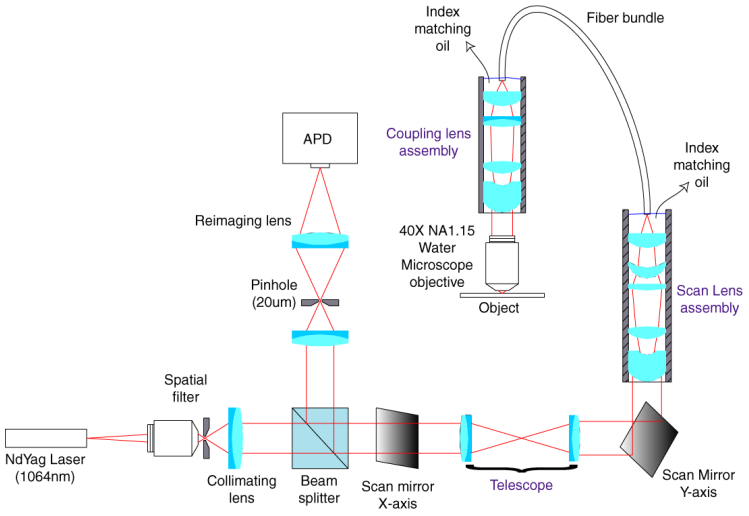

Fig. 1. Diagram of components layout of the fiber confocal reflectance microscope.

A continuous wave Nd:YAG laser (Optomech Ltd.) operating at $\lambda = 1{,}064$ nm serves as the illumination source. The laser light is spatially filtered and collimated before passing through an X-Y scanning system. The light is then delivered onto the object via, in order, the scan lens system, the coherent fiber bundle, the coupling lens system and the microscope objective. Illumination light is focused in the tissue sample to the depth of interest. Light is reflected from the tissue due to variations in index of refraction. The reflected light retraces the same path in reverse until the beam splitter, where it is deflected, passes through a pinhole and a re-imaging lens onto a high-speed avalanche photodiode (APD). Each fiber within the coherent fiber bundle is conjugate to the pinhole thus creating a scanning confocal microscope

#37344 - $15.00 US
Received October 26, 2001; Revised December 13, 2001

system. The laser has a relatively short coherence length compared to the length of the fiber bundle, which prevents possible interference effects between light coming from the object and light specular reflected form the proximal face of the fiber bundle.

The X-axis scan mirror is a resonant scanner (Electro-Optical Products Corporation, model number SC30) that operates at 7.68 kHz with a maximum scan angle of 12 degrees. The Y-axis scan mirror (Cambridge Technology, model number 6800HP) operates at 15 Hz with a maximum scan angle of 17 degrees. The diameter of the coherent fiber bundle (Sumitomo Electric U.S.A., Inc., model number IGN-15/30) is 1.37 mm while each individual fiber has a core diameter of 4.1 μm and the fiber center-to-center distance is approximately 7.1 μm [9]. The microscope objective used is an Olympus UApo 40X, 1.15 numerical aperture (NA) infinity-corrected, water-immersion objective. The telescope, the scan lens, and the coupling lens systems are custom designed and fabricated.

The estimated lateral resolution of the fiber confocal reflectance microscope is approximately 1.8 μm. The lateral resolution is limited by the fiber spacing within the coherent fiber bundle and the magnification factor of the microscope objective and coupling lens combination. The magnification factor of the microscope objective and coupling lens combination is the ratio of their numerical apertures, which is approximately 3.8. Given the fiber spacing of 7.1 μm the lateral resolution can be estimated by:

$$Lateral\ resolution = \frac{Fiber\ spacing}{m_{microscope\ objective\ /\ coupling\ lens}} = 1.8\,\mu m \qquad (1)$$

Maximizing the signal strength relative to the background radiation is an important design consideration since the index mismatch between the nuclei and the cytoplasm is only approximately $\Delta n = 0.05$. This index mismatch translates to a Fresnel reflectance of 0.034%. The low object reflectance requires effective suppression of background radiation. Background radiation originating from stray reflection and scattering is effectively blocked by the pinhole. The pinhole does not block background radiation caused by the specular reflection from the proximal and distal faces of the coherent fiber bundle [10]. The solution that we have adopted involves the use of index matching oil at both coherent-fiber-bundle faces in order to reduce specular reflections from these surfaces. At the distal face the index matching oil matches the index of the fiber cores. At the proximal face the index matching oil matches the average index of the core and the cladding. Specular reflection from the distal face of the fiber bundle is small because the light has to propagate back through the fiber bundle. Specular reflection from the proximal face of the fiber bundle is approximately 0.0025%. Compare to the specular reflection from the proximal end of the fiber bundle, he signal suffers additional loss from fiber coupling, Fresnel reflection loss at the coupling lens and microscope objective, and scattering and absorption in the tissue. The estimated throughput of the signal is approximately two times the throughput of the specular reflected light if the object plane is near the surface. Background subtraction is also used to further reduce these Fresnel reflections.

A two-dimensional (2D) image is built up point-by-point through X-Y scanning of a focused spot across the fiber bundle by means of the scan mirrors. At any given time only one fiber is illuminated and imaged. The object may be translated axially towards or away from the microscope objective to allow imaging of different depths.

3. Telescope and scan lens design

3.1 Requirements

An afocal telescope is needed to couple the two scan mirrors in the setup (see Fig. 1). The X-axis scan mirror and Y-axis scan mirror are mechanically separated and differ in size. Both mirrors need to be positioned at a pupil location of the scan lens because each mirror

#37344 - $15.00 US Received October 26, 2001; Revised December 13, 2001

generates only one direction of scanning. In addition the size of the entrance pupil of the scan lens needs to match the effective size of the Y-axis scan mirror, and the effective size of the Y-axis scan mirror also needs to match the effective size of the X-axis scan mirror. Therefore, the two scan mirrors need to be coupled optically. A telescope is inserted between the two scan mirrors and images the X-axis scan mirror onto the Y-axis scan mirror with the proper magnification factor is required to accomplish the optical coupling.

The scan lens immediately follows the scan mirrors and is used to couple the incident light into individual fibers in the coherent fiber bundle (see Fig. 1). The scan lens has an entrance pupil located at the Y-axis scan mirror to achieve pupil matching with the telescope. The size of the entrance pupil matches the size of the Y-axis scan mirror. The scan lens requires a NA of 0.3 in its image space to match the acceptance NA of the optical fibers. The scan lens must be diffraction limited so that it will only illuminate one fiber at a time to achieve the highest possible coupling efficiency. High coupling efficiency into a single fiber leads to a higher image contrast.

The scan lens needs to be telecentric in image space so the chief ray is parallel to the optical axis at each fiber in the bundle. This condition is necessary for the cone of converging light to have a normal incidence on the fiber. If the telecentricity condition is not satisfied then the coupling efficiency and therefore the image contrast would vary across the fiber bundle.

The field of view (FOV) of scan lens is defined by the FOV of the microscope objective and the magnification factor of the microscope objective and coupling lens combination. For the commercial microscope objective used in present setup (see Fig. 1) the FOV is approximately 250 μm. The magnification factor (m) of the microscope objective and coupling lens combination is 3.8. The FOV of the scan lens system can now be determined to be:

$$FOV_{Scan\,lens} = FOV_{Microscope\,objective} \times m_{microscope\,objective/Coupling\,lens} \cong 1\,mm\,. \qquad (2)$$

3.2 Design

The telescope is constructed using two achromatic doublets. Both achromatic doublets are commercially available from Melles Griot (LA0037 and LA0059). Fig. 2(a) shows the telescope optical design. The focal lengths of the two doublets are 40 mm and 50 mm, respectively. The resultant transverse magnification is 1.25. This magnification factor is chosen to match the size of the entrance pupil of the scan lens to the effective size of the Y-axis scan mirror and the exit pupil of the telescope. The entrance pupil of the telescope system is located at the front focal plane of the f = 40 mm doublet and the exit pupil is located at the back focal plane of the f = 50 mm doublet. The two scan mirrors are positioned at these pupil locations [see Fig. 1(a)].

The scan lens system is constructed with five refractive singlets. The design of the scan lens also takes advantage of off-the-shelf components. Three of its lenses are commercially available: The third lens is from Melles Griot (LPX267), the fourth lens is from Coherent, Inc. (43-3730) and the last lens is a GRADIUM lens (GPX-10-10) [11]. GRADIUM lenses have an index of refraction that varies along the optical axis. The first two lenses are custom made by MediVision [12]. Fig. 2(b) shows the optical layout of the scan lens. The optical clear aperture diameter is 26 mm and total length is approximately 235 mm, as measured from the first lens vertex to the image plane. Detailed prescriptions data for the telescope and scan lens are given in Table 1. This scan-lens design satisfies all of the requirements stated in the previous section. The design may be simplified further if off-the-shelf elements are replaced by additional custom elements.

#37344 - $15.00 US Received October 26, 2001; Revised December 13, 2001

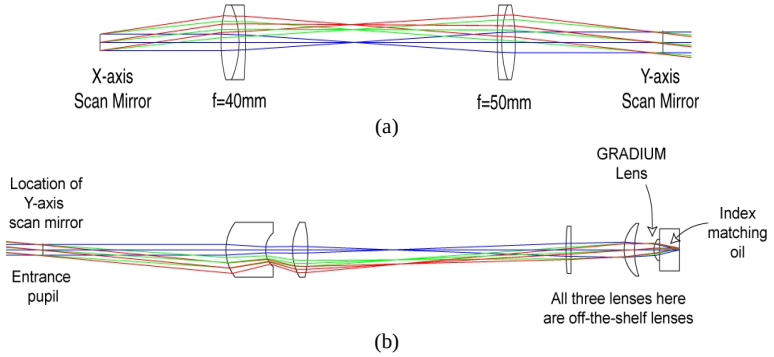

Fig. 2. Telescope and scan-lens designs. Part (a) shows the optical layout of the telescope. Part (b) shows the optical layout of the scan lens assembly. The color of each ray bundle corresponds to a different field position at the coherent fiber bundle, denoted by *h*. Blue rays represent on-axis field position, green rays represent $h = 0.35$ mm, and red rays represent $h = 0.5$ mm.

Table 1. Prescription data for telescope and scan lens

Surf	Comment	Radius (mm)	Thickness (mm)	Glass
OBJECT		Infinity	Infinity	
STOP		Infinity	40	
2	LAO037	27.25	5.94	SSK4A
3		-17.36	2.1	SF8
4		-101.11	83.22	
5		89.35	1.5	SF5
6		22.46	4.46	SK11
7	LAO059	-32.15	48.78	
8		Infinity	95	
9		20	20.62	LAK10
10		10.12	13.97	
11		24.98	8	BK7
12		-57.15	134.02	
13	LPX267	103.74	2.6	BK7
14		Infinity	27.55	
15	43-3730	15.67	5.4	BK7
16		35.12	10.1	
17	GPX-10-10	7.52	3	G14SFN
18		Infinity	10.27	Index matching oil
IMAGE		Infinity		

The telescope and scan-lens system can be designed separately and both have to be well corrected for aberrations. Alternatively, these two optical systems can be designed together so that the aberrations introduced by the telescope can be used to balance the aberrations introduced by the scan-lens system. The latter approach was used here since it will generally lead to a simpler design form. The detailed optical design was executed using the ray trace program ZEMAX [13].

#37344 - $15.00 US Received October 26, 2001; Revised December 13, 2001

3.3 Performance

The performance of the telescope/scan-lens system was first predicted in ZEMAX. The telescope/scan-lens optical system is diffraction limited with a Strehl ratio of 0.97 on axis at 0.72 at the edge of the field [14]. Fig. 3 shows the predicted spot diagrams of the design at three radial positions on the coherent fiber bundle. The RMS spot diameter is approximately 1.3 μm on axis and 2.9 μm at the edge of the field (h = 0.5 mm). The dominating aberration at the edge of the field is coma as can be seen from the shape of the geometric spot diagram (see Fig. 3). The blurred geometric spot is still within diameter of the Airy disc, which is indicated by the circle on the spot diagrams in Fig. 3. The geometric spot size is also smaller than the fiber-core diameter and thus should not cause significant image-contrast degradation.

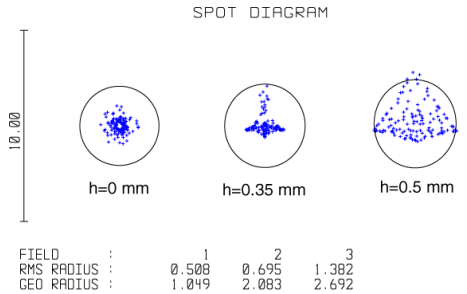

Fig. 3. Geometric spot diagram for the telescope/scan lens system at three different field positions at the coherent fiber bundle, denoted by h. The circle in each diagram represents the size of the diffraction Airy disc. Spot radius values given in the diagram are in micrometers.

The image quality of the telescope/scan lens system was tested experimentally by directly examining the focal spot. Collimated light incident onto the telescope/scan lens system and forms a focal spot at the back focal plane. The focal spot is then examined through a microscope objective. Fig. 4(a) shows the focal spot and its diameter is approximately 3.4 μm. The diffraction Airy Disc diameter is calculated to be:

$$\frac{2.44\lambda}{NA} = 4.3\mu m \tag{3}$$

Therefore, the telescope/scan lens has demonstrated experimentally diffraction-limited performance. The calculated diameter in Eq(3) corresponds to the first zero location of the point spread function (PSF). The measured diameter of the focal spot is smaller than the calculated value. This is because the camera used in the measurement has a finite dynamic range and sensitivity and it is not capable to detect the edge of the focal spot where the intensity is near zero. The ability of the telescope/scan lens system to couple light into a single fiber was also tested. Collimated light is coupled into the fiber bundle using the telescope/scan lens system. Ideally, the telescope/scan lens system will focus light only onto a single fiber. This is demonstrated in Fig. 4(b). Here the distal end of the fiber bundle is shown with only one fiber illuminated by the telescope/scan lens system. This allows maximum image contrast to be achieved.

#37344 - $15.00 US Received October 26, 2001; Revised December 13, 2001

(a) (b)

Fig. 4. Part (a) shows the focal spot formed by the telescope/scan lens system. The spot diameter is approximately 3.4 µm. Part (b) shows the distal end of the fiber bundle when only one fiber is illuminated by the telescope/scan lens. Dotted circles represent the surrounding fibers.

4. Coupling lens design

The functionality of the coupling lens system is similar to that of the scan lens system. It is responsible for coupling illumination from the coherent fiber bundle to the microscope objective and reflected light from the microscope objective into the fiber bundle. Therefore, its entrance pupil must match the size and location of the exit pupil of the microscope objective. The coupling lens has similar performance requirements as the scan lens, specifically the system must be diffraction limited at NA = 0.3 in order to couple light into only one fiber at a time. Finally, the coupling-lens design was derived from the scan-lens design, which explains the similarities in design forms between the two.

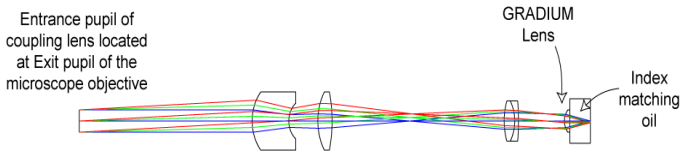

Fig. 5. Optical layout for the coupling lens system. The color of the ray bundle corresponding different field position. Blue rays represent on axis, green rays represent *h*=0.35 mm, and red rays represent h=0.5 mm.

Fig. 5 shows the optical layout of the coupling lens, and Fig. 6 shows its predicted spot diagrams. The optical clear aperture diameter of the coupling lens is 26 mm and total length is approximately 190 mm, as measured from the first lens vertex to the image plane. The detailed surface prescription for the coupling lens is given in Table 2. The RMS spot diameter is approximately 1.5 µm on axis and 2 µm at the edge of the field. The Strehl ratio is 0.99 on axis and 0.88 at the edge of the field. The coupling-lens system is also telecentric in image space for the same reason as is the scan-lens system. The coupling lens system was tested experimentally and its performance is comparable with the telescope/scan lens system. Additionally, the coupling lens is constructed using only four lenses and these are the same lenses that are used for the telescope/scan lens system. Therefore, no new optical elements need to be fabricated. This is a direct benefit resulting from the similarity of the coupling-lens and scan-lens designs.

#37344 - $15.00 US Received October 26, 2001; Revised December 13, 2001

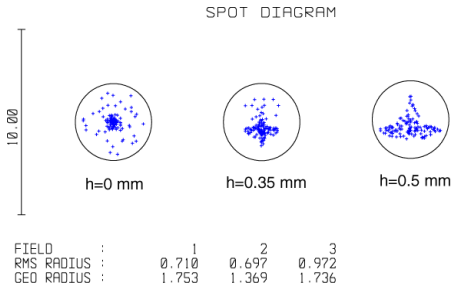

Fig. 6. Geometric spot diagrams for the coupling lens system at three different field positions at the coherent fiber bundle, denoted by *h*. The circle in each diagram represents the size of the diffraction Airy disc. Spot radius values given in the diagram are measured in micrometers

Table 2. Prescription data for telescope and coupling lens

Surf	Comment	Radius (mm)	Thickness (mm)	Glass
OBJECT		Infinity	Infinity	
STOP		Infinity	97.26	
2		20	20.62	LAK10
3		10.12	16.32	
4		24.98	8	BK7
5		-57.15	96.81	
6	LAO037	27.25	5.94	SSK4A
7		-17.35	2.1	SF8
8		-101.11	25.88	
9	GPX-10-10	7.52	3	G14SFN
10		Infinity	11.61	Index matching oil
IMAGE		Infinity		

5. Image data

The FCRM was used to image a resolution target to demonstrate its lateral resolution. The resolution target used is a standard United State Air Force resolution test target. Fig. 7 shows the image of the resolution target taken with the FCRM. The smallest set of bar patterns shown in Fig. 7 has line thickness and spacing of 2.19 μm and it can be resolved. This is comparable with the estimated lateral-resolution value given in Eq. (1). The actual bars on the resolution target are straight. The bars seen in Fig. 7 are distorted. This is due to the intrinsic distortion of the coherent fiber bundle.

#37344 - $15.00 US Received October 26, 2001; Revised December 13, 2001

Fig. 7. Image of resolution target taken with the fiber confocal reflectance microscope. The smallest features have line thickness and spacing of approximately 2 μm.

The axial resolution of FCRM was measured by imaging a plane mirror moved through focus. A strong reflected signal is detected when the mirror is at the focal plane. The reflected signal decreases as the mirror is defocused because the pinhole rejects the defocused light. Fig. 8 shows the reflected signal as a function of defocus. The axial resolution is determined by the profile's FWHM, which is approximately 6 μm.

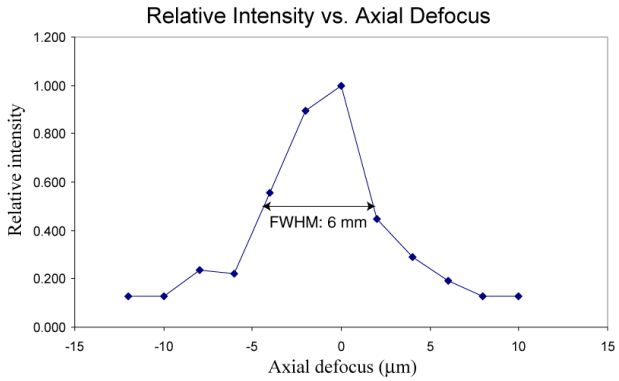

Fig. 8. Reflected signal from imaging a plane mirror as a function of defocus. The FWHM determines the axial resolution and it is approximately 6 μm.

Finally, the FCRM was used to image human cervical biopsy tissue. Fig. 9(a) and Fig. 9(b) show the confocal images of epithelial cells from normal and abnormal cervical biopsies, respective. Both images correspond to an object plane at an approximate depth of 30 μm below the surface. Fig. 9 also demonstrates the optical sectioning capability of the FCRM system. The bright spots are the nuclei and the dark region is the cytoplasm. The index mismatch between the nuclei and cytoplasm is $\Delta n \cong 0.05\text{-}0.07$. A 6% acetic acid solution was used to enhance the image contrast by highlighting the nuclear morphology. Cell nuclei can be clearly resolved in Fig. 9, which provides useful information regards to nuclei size and density as well as nuclear-to-cytoplasmic ratio. For normal cells the nuclear-to-cytoplismatic ratio should be approximately 1:5 while for abnormal cells the ratio is close to 1:1 [5]. The brightness and contrast were adjusted for Fig. 9 to reduce contrast-degrading effect of background radiation due to residual Fresnel reflection from the terminal faces of the fiber

#37344 - $15.00 US Received October 26, 2001; Revised December 13, 2001

bundle. Background subtraction was also performed to enhance contrast in Fig. 9. This representative result demonstrates the sensitivity of the FCRM instrument.

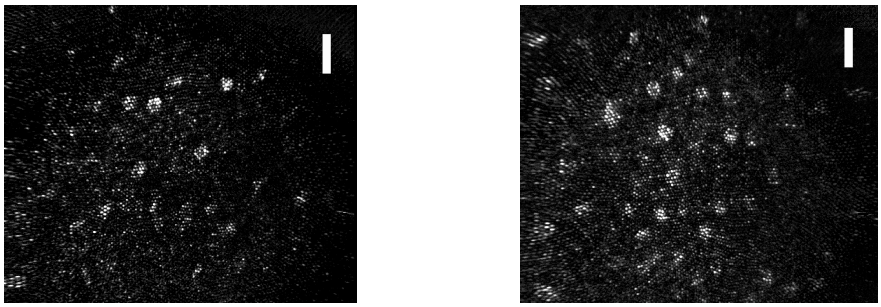

(a) (b)

Fig. 9. Confocal image of epithelial cells from cervical biopsies. Part (a) shows normal tissues and part (b) shows abnormal tissues. Acetic acid solution of 6% concentration was used to enhance the contrast. Scale bar indicates 20 μm.

6. Conclusion and further work

A FCRM designed for detecting pre-cancerous cells in the cervix by *in-vivo* imaging has been designed, built, and tested. The optical subsystems of the FCRM are well corrected for aberrations. Their performance is limited only by diffraction. FCRM has demonstrated a lateral resolution of 2 μm, which is sufficient to resolve cell nuclei. The axial resolution of the FCRM was measured to be approximately 6 μm. Optical sectioning capability has been demonstrated by imaging thick human cervical biopsy tissue. Cell nuclei can be resolved with good contrast. This demonstrates the sensitivity of FCRM. The index mismatch between the cell nuclei and cytoplasm is only $\Delta n = 0.05$ without contrast agent. The ability to resolve cell nuclei is the key in determining the normality of the tissue.

For future work a custom designed and fabricated miniature microscope objective will be used in place of the commercial microscope objective and the coupling lens. This will allow the FCRM to be used endoscopically. The expected diameter of the miniature microscope objective is approximately 7 mm. The ultimate goal is to develop an instrument that will allow noninvasive 3D in-vivo imaging of the cervix for cancer diagnosis.

Acknowledgments

This research was supported by grants from the National Institutes of Health (CA82880). The authors thank the Optical Instrument Shop at the Optical Sciences Center, University of Arizona, for assembly of the scan-lens and coupling-lens systems.

#37344 - $15.00 US Received October 26, 2001; Revised December 13, 2001